Received: 22 March 2023 | Revised: 25 April 2023 | Accepted: 26 April 2023

DOI: 10.1002/pen.26355

RESEARCH ARTICLE

POLYMER ENGINEERING AND SCIENCE WILEY

Thermal stability and curing behavior of acrylate photopolymers for additive manufacturing

Robert Setter[1,2] | **Stefan Schmölzer**[3] | **Natalie Rudolph**[3] | **Elena Moukhina**[3] | **Katrin Wudy**[1,2]

[1]Professorship of Laser-based Additive Manufacturing, Department of Mechanical Engineering, TUM School of Engineering and Design, Technical University of Munich, Garching, Germany

[2]Collaborative Research Center 814 (CRC 814), Friedrich-Alexander University Erlangen-Nuremberg, Erlangen, Germany

[3]NETZSCH-Gerätebau GmbH, Selb, Germany

Correspondence
Robert Setter, Professorship of Laser-based Additive Manufacturing, Department of Mechanical Engineering, TUM School of Engineering and Design, Technical University of Munich, Boltzmannstr. 15, 85748 Garching, Germany.
Email: robert.setter@tum.de

Funding information
Deutsche Forschungsgemeinschaft: SFB 814 "Additive Manufacturing", Grant/Award Number: Project-ID 61375930

Abstract

Next-generation additive manufacturing processes based on UV-curing acrylate photopolymers extend the barriers of functional part production by deploying rapid processing speeds, complex geometries with high resolutions, and an extended material spectrum. Many technologies introduce temperature-dependent curing and decomposition behavior of acrylates to the list of process-related challenges. This investigation targets a comprehensive analysis of the curing behavior and thermal stability of acrylic photopolymers by implementing analyzing techniques like thermogravimetric analysis, Fourier-transform infrared spectroscopy, and differential scanning calorimetry. Significant parameters such as the UV intensity and the isothermal temperature are varied based on the design of experiments. Characteristic evolving gases at elevated temperatures are identified and discussed towards their relevance for the curing process. The calorimetric results demonstrate increasing reaction speeds with elevated UV intensities as well as a restricted accelerating effect of increasing temperatures. The reaction enthalpy proves to be strongly dependent on the chosen temperature. The results represent the base for the comparison of different kinetic curing models in future investigations.

KEYWORDS

additive manufacturing, differential scanning calorimetry, FT-IR, photopolymerization, thermogravimetric analysis

1 | MOTIVATION

Additive manufacturing (AM) of plastics is one of the most promising technologies in the 21st century. Near-unlimited design freedom qualifies the technology for a broad range of industry sectors, such as the medical field, consumer goods, and the automotive industry. In 2021, photopolymers or UV-light activated polymers ranked second behind polymer powders in AM materials sold worldwide, with a market share of 25.2%.[1] This market share can be explained by the utilization of these materials in AM technologies such as Material Jetting and Vat Photopolymerization, which demonstrate a high maturity and distribution within the private sector as well as

industrial applications. Photopolymers usually consist of monomers, oligomers, and photoinitiators, which are essential building elements for radical polymerization. The essential monomers for photopolymers are acrylates, which combine high reactivity, rapid cure rates, and high versatility with the monomer functionality.[2] Owing to these potentials, there is great interest in the utilization of acrylate-based photopolymers within a broad range of AM technologies. This not only includes state-of-the-art AM but also experimental technologies and concepts with increased functionalities and elevated process-related requirements. Extensive research is invested in the field of photolithography technologies and multi-material AM. Multiphoton lithography represents an AM technology based on ultra-short-pulsed laser/material interaction.[3] Challenges for this technology are limited by the lack of heat resistance of the printable materials. Baldacchini et al.[4] and Jian et al.[5] both successfully demonstrate the suitability of acrylic-based photopolymers for use in multiphoton lithography based on geometrical and optical quality criteria. Nguyen et al.[6] additionally consider the impact of different UV-intensities as well as thermal stability and decomposition behavior based on calorimetric and thermogravimetric measurements. A combined approach to analyze and model the curing kinetics with the exploitation of the influence of the process temperature was not considered in any of the aforementioned investigations. Another technology representative for an AM process with elevated process requirements is the novel "Fusion Jetting" (FJ) process. The FJ process is allocated to the multi-material AM sector which requires challenging requirements towards a tailored curing behavior and sufficient thermal stability of acrylate-based photopolymers. What is defined as multi-material AM in today's market is entirely separated into two individual material classes: the combination of either thermoplastics or thermosets.[7,8] First suggested by Wudy et al.,[9] the FJ process represents one of the first AM attempts to simultaneously process thermosets and thermoplastics into multi-material parts. The technology is based on the combination of two powder-based state-of-the-art AM technologies: laser-based powder bed fusion of plastics (PBF-LB/P) and binder jetting (BJT). The challenging requirements for acrylates arise from the necessity of a high-temperature environment for defect-free PBF-LB/P processing. Previous investigations within the field of FJ processing concentrated on experimentally and mathematically describing the impact of the process temperature and the powder conditions on the infiltration behavior, as well as the impact of homogenously dispersed thermoplastic powders on the dynamic mechanical properties of UV-cured thermoset parts.[10,11] The UV curing behavior of the acrylate systems dependent of the temperature as well as the thermal stability in the high-temperature environment within FJ processing has not been analyzed yet.

Considering the state of research described above, the need for an experimentally deepened understanding of the curing kinetics and decomposition behavior of acrylate photopolymers is inevitable. Compared to conventional AM processes, such as Vat Photopolymerization, next-generation AM processes introduce the temperature-dependent curing and decomposition behavior of acrylates to a list of process-related challenges. These challenges must generally be avoided or used as a tool for strategic tailoring of the curing process. This investigation concentrates on the experimental analysis of the thermal decomposition behavior with subsequent calorimetric analysis of the curing behavior of different acrylate systems. In this context, the following key aspects are investigated:

1. The influence of increased isothermal temperatures during UV-curing on the speed and extent of the reaction of the analyzed acrylate systems.
2. The utilization of the UV-intensity as a tool for strategic variation of the curing speed and the degree of cure of the analyzed acrylate systems.

An initial experimental analysis of the thermal stability of the individual materials based on thermogravimetric and spectroscopic measurements is conducted. This helps to gain a deeper understanding of potential temperature-based processing windows and the process-related risks of introducing liquid photopolymers to elevated states of temperature and temperature environments. The analysis includes the characterization of potential evaporating and deteriorating photopolymer components and the evaluation of their importance for the UV-curing process. Further, an experimental analysis of the chemical crosslinking of the individual materials based on calorimetric measurements is performed. For these experiments, strategic variations in the UV intensity and isothermal temperature were conducted. The results represent the base for the model-based investigation of the curing kinetics described in Reference [12]. In the following, a detailed introduction to the materials and methods of this investigation is given.

2 | MATERIALS AND METHODS

2.1 | Materials

The materials used in this investigation are acrylate-based photopolymers with the tradename "UV DLP Firm" and "UV DLP Hard" by the company Photocentric

TABLE 1 Selected material characteristics of Acrylate A and Acrylate B.[13,14]

	Acrylate A tradename: UV DLP firm	Acrylate B tradename: UV DLP hard
Viscosity/mPas	560	230
Tensile strength/MPa	10	15
Tensile modulus/MPa	700	2060
Density/kg/m^3	1180	1190

3D. Both reactive liquids are photopolymers containing diacrylates (volume percentage of 10%–15% for UV DLP Hard; volume percentage of 15%–20% for UV DLP Firm) and dimethacrylates (volume percentage of 50%–70% respectively) as their proprietary building elements.[13,14] The chemical structures of each element can be found in Section 3.1.

Both materials are selected due to their profound mechanical properties after curing, fast curing speeds, and sufficient controllability of the viscosity behavior through temperature increase. The infiltration behavior within different polymer powders and the rheological behavior at elevated temperatures have already been described in previous investigations.[10] In comparison, the materials differentiate mostly in their viscosity and the mechanical properties of the crosslinked parts. Selected values can be found in Table 1. On a chemical level, the difference between both materials is the presence of a non-specified "multifunctional acrylate" as a proprietary building element within "UV DLP Hard", with volume percentages between 5% and 10%. For simplification and better representation in diagrams and tables, "UV DLP Firm" and "UV DLP Hard" are referred to as "Acrylate A" and "Acrylate B" respectively throughout this investigation.

2.2 | Methods

2.2.1 | Thermogravimetric analysis (TG) with in-situ Fourier-transform infrared spectroscopy (FTIR)

For this investigation, a PERSEUS® TG 209 F1 Libra® thermogravimetric analyzer (NETZSCH, Germany) is utilized for analyzing the decomposition behavior of Acrylate A and Acrylate B at elevated temperatures. Fully cured as well as liquid samples of approximately 40 mg are placed in aluminum crucibles. The heating is performed under a nitrogen atmosphere, starting at 30°C with a heating rate of 10 K/min, followed by an isothermal temperature of

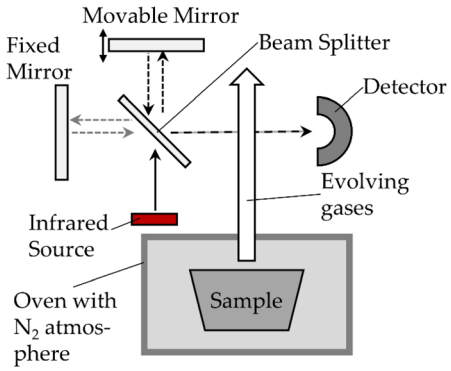

FIGURE 1 Thermogravimetric Analysis (TGA) combined with Fourier-transform infrared spectroscopy (FT-IR).

TABLE 2 Experimental parameters for UV-DSC measurements of Acrylate A and Acrylate B liquid samples.

Isothermal temperatures T_{iso}/°C	30, 90, 150
Soak time t_{soak}/min (for $T = 30$°C $t_{soak} = 0$)	10
Heating rate/K/min	5
Cooling rate/K/min	20
UV-Intensities/mW/cm^2	7.5, 15, 30, 60
Radiation time t_{UV}/min	10
Delay before irradiation start/s	5

200°C for >30 min. The maximum temperature of the program is limited to 200°C. To gather increased information about the so-called "evolved gases" originating from the samples, the thermogravimetric analyzer is paired with in-situ Fourier-transform infrared spectroscopy (FT-IR). For this investigation, the term "evolved gases" defines a gas composition caused by the potentially intercorrelated presence of decomposition and evaporation effects of a material under the influence of elevated temperatures. The FT-IR spectrometer (Bruker Optics, USA) is then used to examine the so-called fingerprint (absorption spectrum in a wavenumber area between 400 and 4000 cm^{-1}) of the evolved gases. For this, the detector of the FT-IR is located above the crucible of the TGA, causing the gas stream to pass between the detector and the beam splitter. A simplified schematic representation of the entire set-up can be seen in Figure 1.

2.2.2 | Differential scanning calorimetry (DSC) with UV-light source (UV-DSC)

With differential scanning calorimetry (DSC) the potential of spontaneous thermal curing of Acrylate A and Acrylate B is examined. Liquid samples of both materials with a mass of approximately 10 mg are analyzed on a

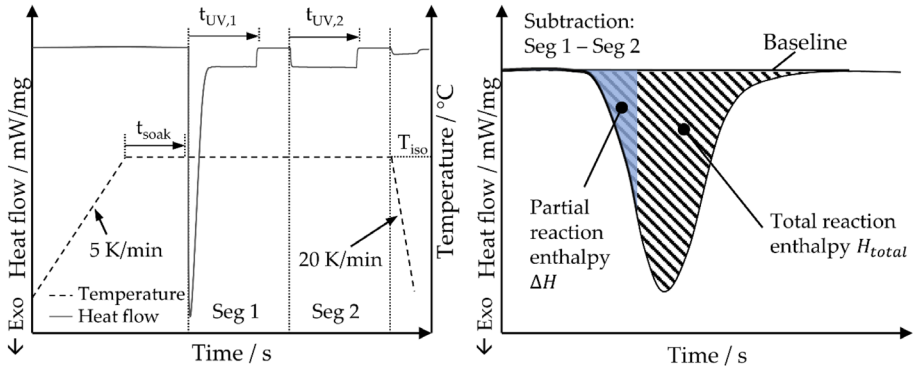

FIGURE 2 Schematic temperature and UV radiation program with isothermal segments Seg 1 and Seg 2 (left diagram); Curve subtraction of segments Seg 1 and Seg 2 with resulting heat flow and integrally determined specific heat with a linear baseline (right diagram).

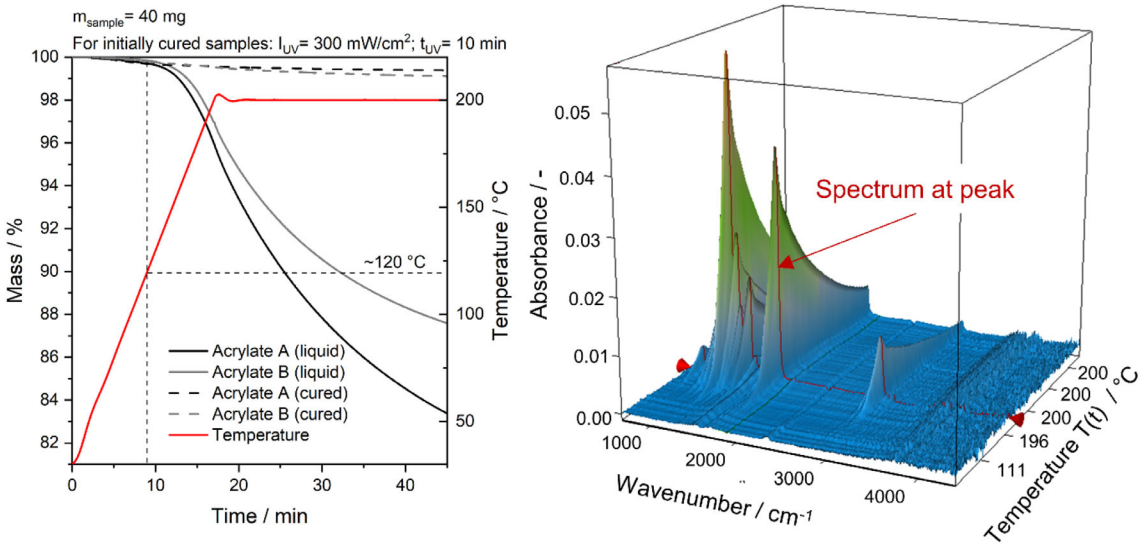

FIGURE 3 TG analysis of Acrylate A and Acrylate B (left) and respective 3-dimensional representation of FTIR spectra of the evolved gases of liquid Acrylate A dependent on the wavenumber and the temperature over time (right) at a heating rate of 10 K/min, followed by an isothermal stage at 200°C for 30 min.

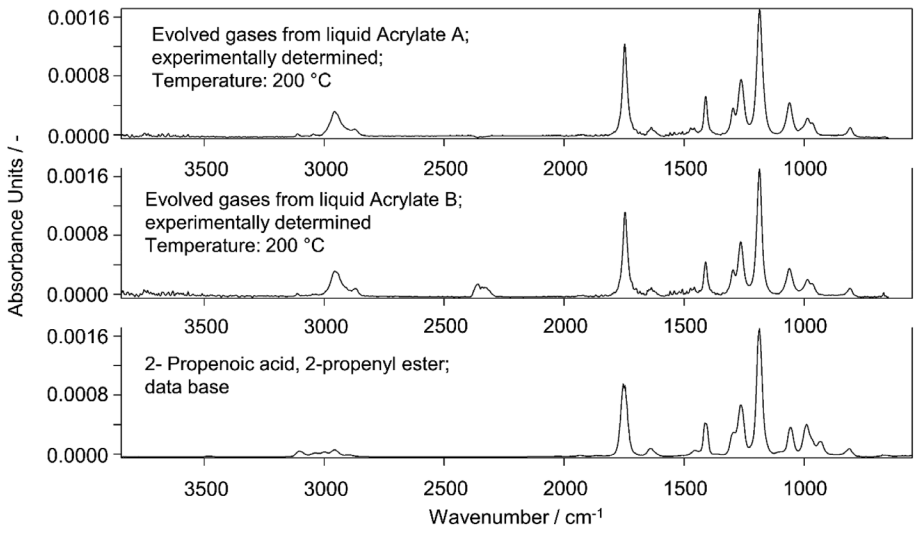

FIGURE 4 Comparison of the characteristic absorbance spectra of the evolved gases from liquid Acrylate A and liquid Acrylate B samples towards the database spectra of 2-propenoic acid, 2-propenyl ester[22] (database spectra extracted from BRUKER analysis software; Comparison at 200°C).

DSC 214 Polyma (NETZSCH, Germany). Each sample is heated from −120°C to 250°C with a heating rate of 10 K/min for determination of potential curing.

To analyze the curing behavior and the exothermic heat flow during UV-curing at different temperatures, DSC with a UV light source (UV-DSC) is used. Liquid

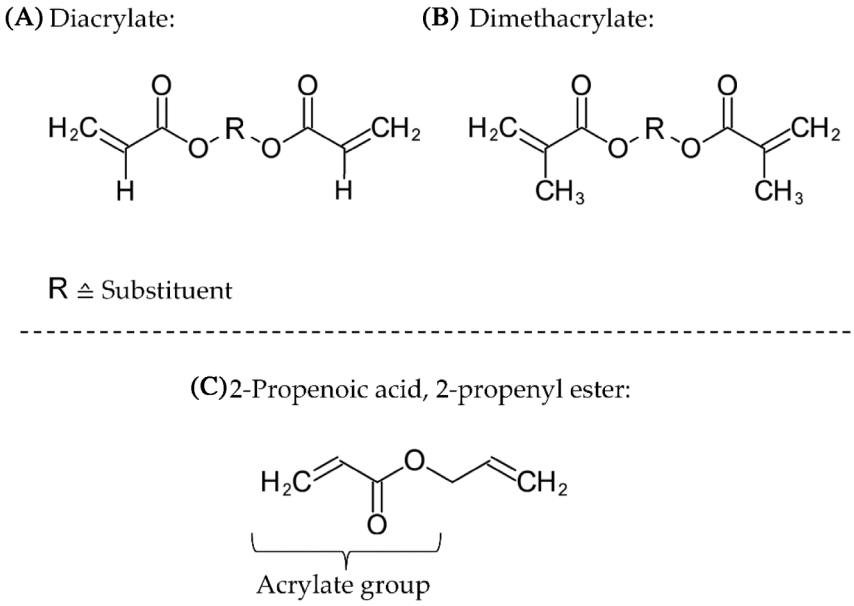

FIGURE 5 Chemical structure of (A) diacrylates and (B) dimethacrylates as proprietary building elements of Acrylate A and Acrylate B compared to the chemical structure of (C) 2-propenoic acid, 2-propenyl ester.

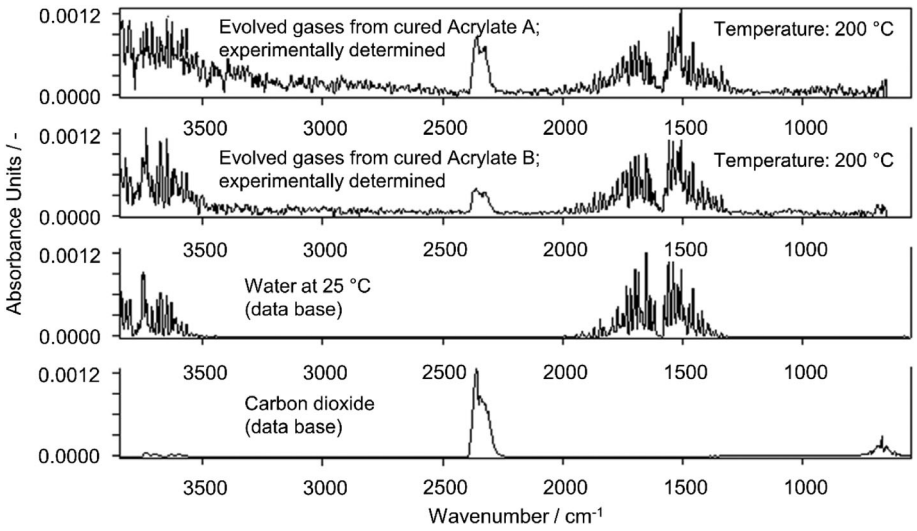

FIGURE 6 Comparison of the characteristic absorbance spectra of the released gases by fully cured Acrylate A and fully cured Acrylate B towards the database spectra of water at 25°C[22] and carbon dioxide[22] (database spectra extracted from BRUKER analysis software; Comparison at 200°C).

Acrylate A and Acrylate B samples with a mass of 5 mg +/−0.02 are analyzed with a Photo-DSC 204 F1 Phoenix (NETZSCH, Germany) under a nitrogen atmosphere. The used UV-light source is an OmniCure® S 2000 (Lumen Dynamics Group, Kanada) with a split light guide. Each liquid sample is pipetted into aluminum crucibles and is weighed before and after DSC analysis to gather information about potential mass loss during the temperature and UV treatment. Previous investigations successfully demonstrated the suitability of UV-DSC for the analysis of the curing behavior of photopolymers for example Bachmann et al.[15] and Jiang et al.[16] Using UV-DSC, it is possible to depict the average curing behavior of the entire photopolymer sample, which is not applicable to methods such as FT-IR. In the case of FT-IR, the detectable curing is restricted to a depth of approximately 2 µm because of the limited infiltration depth of the infrared light within the sample.[17–19] Kardar et al.[20] and Rusu et al.[18] investigated the influence of negative to medium temperatures up to 85°C as well as different atmospheres (nitrogen and oxygen) on the curing behavior of photopolymers combing acrylates and epoxies. The UV-intensities were also varied between 2 and 80 mW/cm^2. In both investigations, increased temperatures and UV-intensities respectively led to accelerated curing. The thermal stability was not analyzed.

As summarized in Table 2, UV-intensities of 7.5, 15, 30, and 60 mW/cm^2 at isothermal temperatures of 30, 90, and 150°C are analyzed for this investigation. The detailed temperature program is depicted schematically in Figure 2. Each sample is exposed to UV-light twice for 10 min for later curve subtraction (Figure 2 left and right). The subtraction allows the creation of a horizontal baseline (Figure 2 right) and acts as a verification for complete

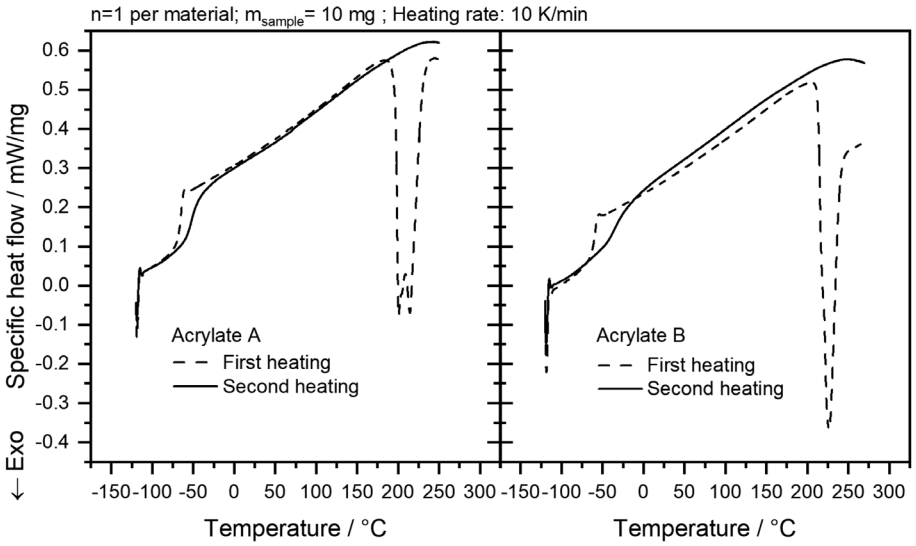

FIGURE 7 DSC analysis of liquid Acrylate A and Acrylate B samples without UV-curing with inclusion of both heating cycles (first and seconding heating) for better interpretation of potential curing.

curing of the sample. Before UV-light activation, soak times of 10 min are included before the isothermal temperatures of 30, 90, and 150°C. All heating rates are 5 K/min and the cooling rates 20 K/min. A 5 s delay is included before each UV-treatment. The results of the DSC and UV-DSC measurements are analyzed towards the specific heat flow and the reaction enthalpy during the exothermal curing reaction. The amount of specific heat released was calculated by integrating the curve based on a specifically selected baseline for integration. For this investigation, a linear baseline is considered for all measurements.

To describe the conversion achieved during the curing reaction the so-called degree of cure is calculated as follows[21]:

$$\alpha = \frac{\Delta H}{H_{total}} = \frac{\int_{t_{start}}^{t} \dot{Q}(t)dt}{H_{total}} \quad (1)$$

The achieved conversion α is the ratio between the partially emitted exothermic amount of specific heat ΔH and the total amount of reaction enthalpy available H_{total} (compare Figure 2). In the case of DSC or UV-DSC measurements of this investigation, H_{total} is calculated regarding the enthalpy of each individual curve. Accordingly, ΔH is described as the integral of the specific heat flow $\dot{Q}(t)$ over the time t from the start of the reaction t_{start}.

3 | RESULTS AND DISCUSSION

3.1 | Thermal stability and decomposition behavior

For this investigation "thermal stability" is defined according to ASTM E2550, which establishes the onset temperature as well as the overall curve progression and extent of mass loss during temperature increase as significant aspects for result description. Figure 3 (left) shows a mass loss at temperatures between approximately 50 and 120°C for all analyzed samples. The mass loss up to 120°C is around 0.05% for all samples. With further increasing temperatures, the liquid samples experience an accelerated mass loss, while the cured samples illustrate a steady decline in mass. The onset of both liquid samples is approximated at 155–165°C. After an isothermal stage at 200°C of 30 min, the remaining mass of the cured samples lies between 98% and 98.5%. The mass loss of Acrylate B is significantly lower than of Acrylate A, indicating a higher thermal stability in its liquid state. This behavior can most likely be correlated to the presence of the additional "multifunctional acrylate" within liquid Acrylate B as described in Section 2.1 and a therefore lower presence of potentially more unstable diacrylates. Following the isothermal stage at 200°C for 30 min, the liquid Acrylate A sample experiences a remaining mass around 83%, while the mass of Acrylate B is approximately 87%. Thus, 17% and 13% of the material was decomposed, respectively.

To understand the composition of the eluded materials and their potential significance for the curing process, the gathered in-situ FT-IR results simultaneous to the TG analysis are analyzed. The results can be seen in Figure 3 (right), Figure 4, and Figure 6. In Figure 3 (right), the absorbance behavior of the evolved gases of the liquid materials is exemplified through the extraction of the absorbance spectra of liquid Acrylate A. Indicated by the red line is the absorbance spectrum at the maximum amplitude of the absorption spectrum at a temperature of 200°C. Characteristic peaks can be found between wavenumbers of 500 and 2000 cm^{-1} and at 3000 cm^{-1}.

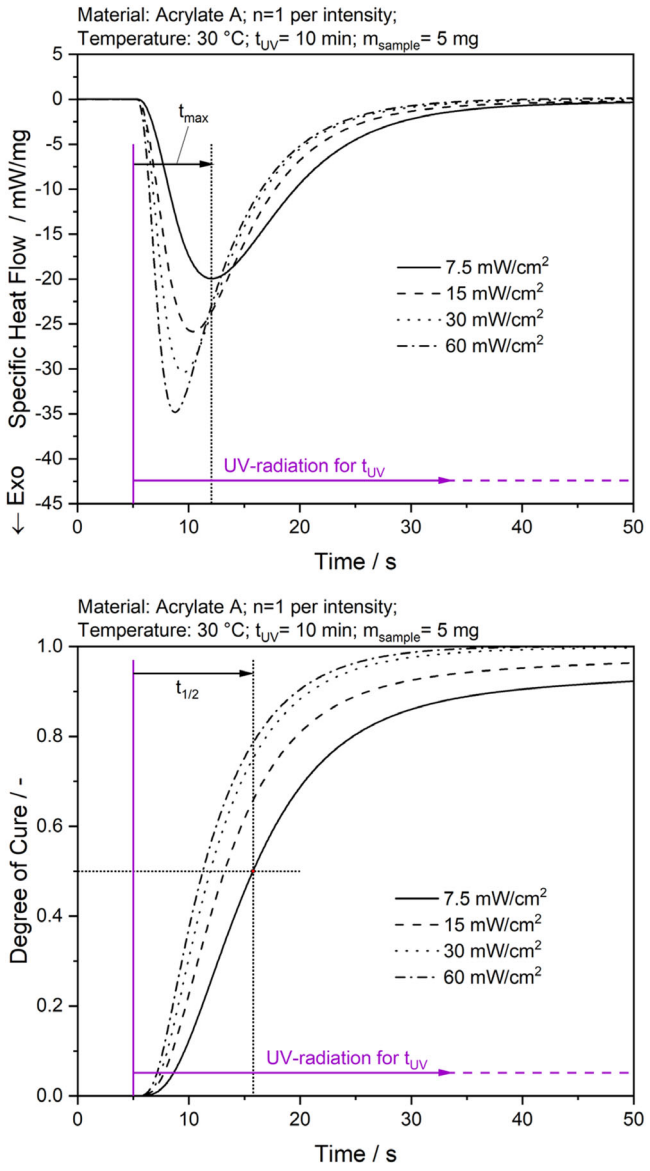

FIGURE 8 Impact of the variation of the UV-intensity on the specific heat flow (above) as well as on the conversion curve of the curing reaction of Acrylate A at an isothermal temperature of 30°C with exemplary determination of the time t_{max} until the highest curing reaction rate is reached and the half-time $t_{1/2}$ of the curing reaction.

The detailed characteristic spectra of liquid Acrylate A and Acrylate B samples can be seen in Figure 4.

Figure 4 shows nearly identical fingerprints for both materials. The main difference is a characteristic peak for Acrylate B at approximately 2300 cm^{-1}, indicating the presence of carbon dioxide[22] (compare Figure 6). Otherwise, the eluded materials show the highest similarity to the solvent "2-propenoic acid, 2-propenyl ester" or "Allyl acrylate"[22] with the following chemical structure:

The presence of the evolved gas most likely correlates to the decomposition and/or evaporation of one of the proprietary building elements of Acrylate A and Acrylate B presented in Figure 5. The shared presence of the acrylate group of 2-propenoic acid, 2-propenyl within the chemical structure of diacrylates supports this hypothesis (compare Figure 5). As can be seen in Figure 6, the spectral fingerprints of the cured materials do not indicate the presence of 2-propenoic acid, 2-propenyl ester. Instead, gases released from both materials indicate water and carbon dioxide predominantly.[22]

3.2 | Experimental analysis of the curing behavior

3.2.1 | Thermally activated curing

To examine the thermal behavior and potential curing of the acrylate-based photopolymers, DSC measurements are performed on Acrylate A and Acrylate B samples. The thermograms are illustrated in Figure 7. Both heating steps are presented, without the subtraction of the individual segments.

The DSC results indicate no curing at temperatures below 175°C. Near 200°C, Acrylate A starts to cure without the use of a UV light source. Similar behavior is visible for Acrylate B starting at approximately 210°C. The curing is indicated by the visible exothermal peak that is present during the first heating of both materials. The second heating indicates a distinct glass transition for both materials at approximately −40°C but no exothermal peak at higher temperatures. In addition, the first and second heating cycles exhibited near-identical exothermal behavior between temperatures of 0 and 180°C. In comparison to the results of UV crosslinking presented in Section 3.2.2, the amount of heat dissipated during the thermally activated exothermal reaction is significantly lower by a factor of approximately 20. The reaction enthalpies through thermal crosslinking of Acrylate A and Acrylate B are approximated at 15–16 J/g with a linear baseline.

3.2.2 | Impact of UV-intensity and different isothermal temperatures on characteristic reaction times

Because of the similarity of the effects and reaction types of both materials, the UV-DSC results presented in the diagrams below are limited to Acrylate A alone. The comprehensive UV-DSC results of Acrylate A and Acrylate B can be found in the Figure A1. The impact of different UV-intensities at an isothermal temperature of 30°C is presented in Figure 8. Only the first 50 s of the reactions

TABLE 3 Time t_{max} until the highest curing reaction rate is reached, half-time $t_{1/2}$ of the curing reaction, and total reaction time t_{total} of the curing reaction for Acrylate A and Acrylate B dependent of the UV-intensity and the isothermal temperature.

	30°C		90°C		150°C	
UV-intensity/mW/cm²	**Acrylate A**	**Acrylate B**	**Acrylate A**	**Acrylate B**	**Acrylate A**	**Acrylate B**
Time at maximum reaction rate t_{max} at different isothermal temperatures/s						
7.5	7.1	6.1	5.2	4.9	4.5	4.4
15	5.4	5.2	4.4	4.3	3.9	3.8
30	4.5	4.3	3.7	3.5	3.4	3.2
60	3.8	3.5	3.0	3.0	2.9	2.8
Curing half-time $t_{1/2}$ at different temperatures/s						
7.5	10.8	10.7	7.9	8.4	7.5	8
15	8.2	8.9	6.8	6.2	6.6	6.9
30	6.9	7.5	6.1	7.2	5.7	5.9
60	6.3	6.3	5.2	5.4	5	5.2
Total reaction time t_{total} at different temperatures/s						
7.5	530	431	470	589	451	650
15	392	277	171	548	396	482
30	71	133	78	443	85	325
60	42	50	38	166	40	247

are presented. For all measurements, t_{max} is determined, which represents the time after UV light activation until the individual DSC curves reach their maximum reaction rate. Comprehensive t_{max} values for all UV-DSC measurements and materials can be found in Table 3.

Figure 8 and Table 3 illustrate the influence of the UV-intensity and isothermal temperature on the time with the highest reaction rate t_{max}. Increasing the UV intensities led to a decrease in t_{max} for all examined temperatures and materials, indicating that the highest reaction rate was reached earlier. The progression of the values indicates an exponential decay for increasing UV-intensities (compare Figure 10 at the end of Section 3.2.2). Furthermore, t_{max} decreases for elevated isothermal temperatures. With increasing temperature, the mobility of the monomer units is increased, which goes along with a higher probability of collision between the monomers and thus a higher probability of crosslinking. The impact of the isothermal temperature on t_{max} is illustrated for a constant UV-intensity of 15 mW/cm² in Figure 9. The accelerating behavior through the increase of the UV-intensity and the isothermal temperature is presumably correlated to the collision theory initially proposed by Trautz[23] and Lewis[24] individually. By increasing the UV light intensity, the number of photons that interact with the photopolymer is increased, resulting in a higher probability for the photons to collide with the photoinitiators of the reactive liquids, leading to a faster initiation and progression of the reaction. Through the

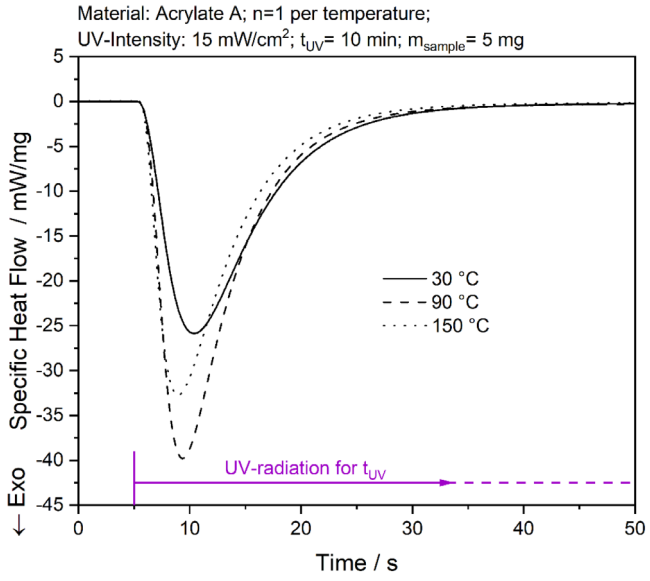

FIGURE 9 Impact of the variation of the isothermal temperature on the specific heat flow of Acrylate A for a UV-intensity of 15 mW/cm².

increase of the temperature, the molecule movement is accelerated and the average kinetic energy per molecule is increased, which subsequently increases the number of collisions that have enough energy. Therefore, an increase in both parameters benefits the probability of molecular collisions of sufficient energy and subsequent

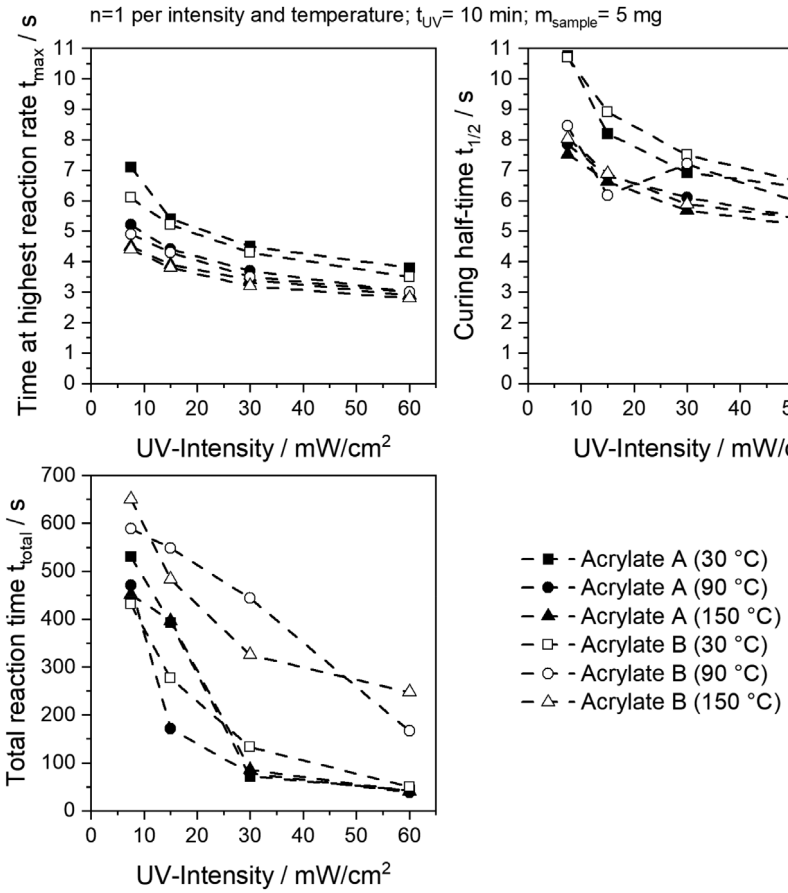

FIGURE 10 Time with the highest reaction rate t_{max}, curing half-time $t_{1/2}$, and total reaction time t_{total} of the curing reaction for Acrylate A and Acrylate B dependent of the UV-intensity and the isothermal temperature.

curing of the proprietary building elements to the polymer chains.

Figure 8 shows the curing conversion or rather the progress of the degree of cure (compare Equation (1)) and curing half-time $t_{1/2}$, which is the time until curing conversion reaches 50% based on the UV-DSC results presented in Figure 8. Comprehensive $t_{1/2}$ values for all UV-DSC measurements and materials can be found in Table 3.

Like the t_{max} values, the curing halftime $t_{1/2}$ of both materials demonstrates an accelerated behavior for increasing UV-intensities and temperatures which is correlated to the collision theory described above. The progression of the values indicates an exponential decay for increasing UV-intensities (compare Figure 10 at the end of Section 3.2.2).

For all materials analyzed, complete curing (Degree of cure of 100%) is achieved for the selected parameters. The total reaction time t_{total} is determined, which describes the time until a degree of cure of 100% is reached. The comprehensive results of t_{total} for all UV-DSC measurements and materials can be found in Table 3.

As illustrated in Table 3, the UV-intensity has an accelerating impact on the total duration of the exothermal reaction t_{total}. The progression of the values partially indicates an exponential decay for increasing UV-intensities (compare Figure 10). Only for Acrylate B at temperatures of 90°C the shape of the curve differentiates. After UV-light activation, the curing of the sample prolongs between 30 and 40 s and up to 650 s depending on the intensity. For increasing isothermal temperatures t_{total} demonstrates inconsistent behavior dependent of the material. For Acrylate A, the isothermal temperature marginally impacts the duration of t_{total} with the highest fluctuations at UV-intensities of 7.5 and 15 mW/cm^2. For Acrylate B however, t_{total} is increased for all UV-intensities by raising the isothermal temperature from 30 to 90°C. Between 90 and 150°C however, the behavior of t_{total} again becomes inconsistent. For 7.5 and 60 mW/cm^2, an increase is visible and for 15 and 30 mW/cm^2 a decrease. Overall, Acrylate A shows significantly smaller t_{total} values compared to Acrylate B, which presumably correlates with the elevated decrease of proprietary building elements of Acrylate A as described in Section 3.1.

3.2.3 | Impact of different UV-intensities and isothermal temperatures on the reaction enthalpy

Table 4 shows the integrally determined reaction enthalpy H_{total} (compare Equation (1)) at different temperatures

TABLE 4 Reaction enthalpy during crosslinking of Acrylate A and Acrylate B samples at different UV-intensities and temperatures.

	Reaction enthalpy at different temperatures/J/g					
	Acrylate A			Acrylate B		
UV-intensity/mW/cm^2	30°C	90°C	150°C	30°C	90°C	150°C
7.5	286	346	286	253	331	316
15	282	342	287	253	322	314
30	273	337	273	249	333	313
60	286	335	272	251	325	313
Average	282	340	279	251	327	314

for Acrylate A and Acrylate B. By analyzing the amount of heat dissipated, the UV-intensity cannot be correlated conclusively to the reaction enthalpy. In individual cases, a slight decline of the reaction enthalpy can be detected with increasing UV-intensity. However, the decline is inconsistent and is declared as non-significant in comparison to the measurement uncertainty of the UV-DSC measurements. For this investigation, the reaction enthalpy is assumed non-correlative to the UV-intensity for all materials analyzed. The impact of the temperature is highly interrelated to the reaction enthalpy: $H_{total}(30°C) < H_{total}(90°C) > H_{total}(150°C)$. The dependence is the case for all materials analyzed, but most significant for Acrylate A. The highest reaction enthalpy for both materials can be found at 90°C, indicating the highest chemical curing of the three temperatures analyzed. For 30 and 90°C respectively, the amount of heat dissipated through Acrylate A is approximately 30 and 13 J/g higher than for Acrylate B. At 150°C, the reaction enthalpy decreases significantly for both materials compared to 90°C. For Acrylate A the decrease is the highest with 61 J/g and for Acrylate B with 13 J/g. Considering the standard deviation of the measurements, Acrylate A experiences the highest fluctuation in reactive behavior at this temperature.

A hypothesis for the above-described temperature-based behavior of both materials is based on two superimposing effects:

a. The acceleratory impact of the temperature on the reaction speed.
b. The material decomposition at elevated temperatures.

Aspect (a) again correlates with collision theory, as described in Section 3.2.2. Through the increase of the temperature, the molecule movement is accelerated and the average kinetic energy per molecule is increased, which subsequently increases the number of collisions that have enough energy. This represents a hypothesis for the increase of reaction enthalpy from 30 to 90°C and the shortening of the reaction time. Aspect (b) represents

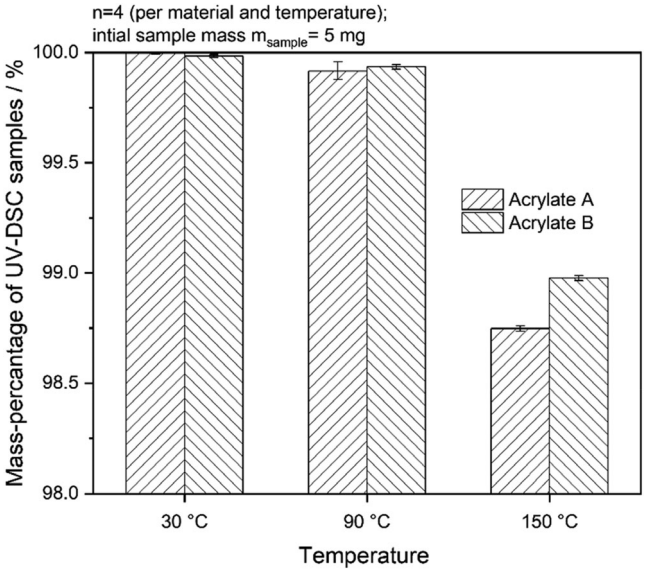

FIGURE 11 Average mass percentage of UV-DSC samples after the measurement with an initial mass of 5 mg at different isothermal temperatures for Acrylate A and Acrylate B respectively.

a potentially negative aspect of the reaction that must be considered, which is represented by the mass loss on UV-DSC samples at different temperatures, as shown in Figure 11. The diagram shows the mass percentage of the UV-DSC samples of Acrylate A and Acrylate B after being exposed to different isothermal temperatures. Visible for both materials is a significant mass-loss of 1%–1.5% respectively at temperatures of 150°C, with Acrylate A experiencing the higher mass loss. This behavior can be directly correlated to the results described in Section 2.2.1. The increased mass loss for Acrylate A correlates well with the obtained TG results (compare Section 2.2.1; Figure 3 (left)). As described before, the detected 2-propenoic acid, 2-propenyl ester is potentially caused by decomposition and/or evaporation of a proprietary building element. If this is the case, the reduction in the component potentially explains the decrease in the reaction enthalpy. Consequently, for curing at 150°C, the beneficial

effect represented by aspect (a) above is overshadowed by the negative effect described through aspect (b).

4 | CONCLUSION

This investigation successfully demonstrated a comprehensive analysis of the curing behavior and thermal stability of acrylic photopolymers for use in next-generation AM technologies. Thermogravimetric analysis, Fourier-transform infrared spectroscopy, and differential scanning calorimetry were utilized to analyze the thermal stability and curing behavior. The UV intensity and isothermal temperature varied according to the experimental design. Combinations of isothermal temperatures of 30, 90, and 150°C with UV-intensities of 7.5, 15, 30, and 60 mW/cm^2 have been analyzed. Besides their difference in chemical constitution, the materials analyzed (Acrylate A and Acrylate B) show nearly identical behavior for the curing behavior in dependence of the parameters varied. Increasing UV-intensities and thereby the number of impacting photons, significantly increases the reaction rate. The highest reaction rates are reached before 50% of the conversion is reached. The increased isothermal temperatures during UV-curing proved to have an enhancing as well as an impeding impact on the speed and extent of the acrylate reaction due to parallel promotion of molecular movement and material decomposition. An accelerating impact of the temperature and an increase of the reaction enthalpy is only visible from 30 to 90°C. For 150°C, the reaction speeds are comparable to 90°C and the total reaction enthalpy is lowered. It was demonstrated that the UV intensity can be strategically utilized and varied to impact the curing speed and degree of cure of the reactive liquids. With simultaneous TG and FT-IR analysis, it was possible to characterize the thermal stability of the materials analyzed including the constitution of evolving gases. 2-propenoic acid, 2-propenyl ester was identified as a temperature-sensitive and volatile component originating from the liquid state of both materials analyzed, potentially impacting the speed and extent of the curing reaction. The individual mass loss was the highest for Acrylate A compared to Acrylate B and the decomposition/evaporation started at temperatures above 120°C, which presumably correlates with the increased content of volatile diacrylates within Acrylate A. The results of subsequently performed thermal DSC measurements pointed out the ability of spontaneous curing for both materials at higher temperatures above 175°C. With UV-DSC measurements the progression of the specific heat flow and the reaction enthalpy during polymer curing for different UV-intensities and isothermal temperatures was investigated. The reaction enthalpy proved to be significantly sensitive to the chosen isothermal temperature, experiencing an increase by increasing the isothermal temperature from 30 to 90°C as well as a decrease by increasing the temperature from 90 to 150°C. However, increasing the isothermal temperature had an overall accelerating impact on the reaction speed for both materials, which could be predominantly shown for the halftime of curing and the time until the highest reaction rate was reached. In the case of UV intensity, the impact of the parameter on the reaction enthalpy was insignificant. For all UV-intensities investigated, it was possible to achieve a maximum degree of cure within the duration of UV-light activation. Overall, the results of this investigation represent fundamental insights required for the successful utilization as well as experimentally corroborated and error-free performance of acrylate materials within a processing environment of next-generation AM systems. The results represent the base for the model-based investigation of the curing kinetics described in Reference [12].

ACKNOWLEDGMENTS

The authors gratefully acknowledge Deutsche Forschungsgemeinschaft (DFG, German Research Foundation) for funding in the framework of SFB 814 "Additive Manufacturing" TP B7. Open Access funding enabled and organized by Projekt DEAL.

DATA AVAILABILITY STATEMENT

The data that support the findings of this study are available from the corresponding author upon reasonable request.

ORCID

Robert Setter https://orcid.org/0000-0003-2166-2794
Natalie Rudolph https://orcid.org/0000-0003-2899-3422
Katrin Wudy https://orcid.org/0000-0002-3384-4651

REFERENCES

1. Wohlers report – 3D printing and additive manufacturing global state of industry. Wohlers Associates. 2022.
2. Ravve A. *Light-Associated Reactions of Synthetic Polymers*. Springer; 2006. https://doi.org/10.1007/0-387-36414-5
3. LaFratta CN, Fourkas JT, Baldacchini T, Farrer RA. Multiphoton fabrication. *Angew Chem Int Ed*. 2007;46(33):6238-6258.
4. Baldacchini T, LaFratta CN, Farrer RA, et al. Acrylic-based resin with favorable properties for three-dimensional two-photon polymerization. *J Appl Phys*. 2004;95(11):6072-6076.
5. Jiang L, Xiong W, Zhou Y, et al. Performance comparison of acrylic and thiol-acrylic resins in two-photon polymerization. *Opt Express*. 2016;24(12):13687-13701.
6. Nguyen LH, Straub M, Gu M. Acrylate-Based Photopolymer for Two-Photon Microfabrication and Photonic Applications. *Adv Funct Mater*. 2005;15(2):209-216.

7. Zheng Y, Zhang W, Baca Lopez DM, Ahmad R. Scientometric analysis and systematic review of multi-material additive manufacturing of polymers. *Polymers*. 2021;13:1957.
8. García-Collado A, Blanco JM, Gupta MK, Dorado-Vicente R. Advances in polymers based multi-material additive-manufacturing techniques: state-of-art review on properties and applications. *Addit Manufact*. 2022;50:102577.
9. Wudy K, Drummer D. Infiltration behavior of thermosets for use in a combined selective laser sintering process of polymers. *JOM*. 2019;71(3):920-927.
10. Setter R, Riedel F, Peukert W, Schmidt J, Wudy K. Infiltration behavior of liquid thermosets in thermoplastic powders for additive manufacturing of polymer composite parts in a combined powder bed fusion process. *Polym Compos*. 2021;42(10):5265-5279.
11. Setter R, Stichel T, Schuffenhauer T, Kopp S-P, Roth S, Wudy K. Additive manufacturing of multi-material polymer parts within the collaborative research center 814. In: Reisgen U, Drummer D, Marschall H, eds. *Enhanced Material, Parts Optimization and Process Intensification*. Springer International Publishing; 2021:142-152.
12. Setter R, Schmölzer S, Rudolph N, Moukhina E, Wudy K. Modeling of the curing kinetics of acrylate photopolymers for additive manufacturing. *Polym Eng Sci*. 2023;63(7):2149-2168. https://doi.org/10.1002/pen.26353
13. Photocentric-Group. UV DLP Hard Safety Datasheet. 2022.
14. Photocentric-Group. UV DLP Firm Safety Datasheet. 2022.
15. Bachmann J, Gleis E, Schmölzer S, Fruhmann G, Hinrichsen O. Photo-DSC method for liquid samples used in vat photopolymerization. *Anal Chim Acta*. 2021;1153:338268.
16. Jiang F, Drummer D. "Curing Kinetic Analysis of Acrylate Photopolymer for Additive Manufacturing by Photo-DSC". *Polymers*. 2020;12(5):1080. https://doi.org/10.3390/polym12051080
17. Esposito Corcione C, Malucelli G, Frigione M, Maffezzoli A. UV-curable epoxy systems containing hyperbranched polymers: kinetics investigation by photo-DSC and real-time FT-IR experiments. *Polym Test*. 2009;28(2):157-164.
18. Rusu MC, Block C, Van Assche G, Van Mele B. Influence of temperature and UV intensity on photo-polymerization reaction studied by photo-DSC. *J Therm Anal Calorim*. 2012;110(1):287-294.
19. Kousaalya AB, Ayalew B, Pilla S. Photopolymerization of acrylated epoxidized soybean oil: a photocalorimetry-based kinetic study. *ACS Omega*. 2019;4(26):21799-21808.
20. Kardar P, Ebrahimi M, Bastani S. Influence of temperature and light intensity on the photocuring process and kinetics parameters of a pigmented UV curable system. *J Therm Anal Calorim*. 2014;118(1):541-549.
21. Haines PJ, Reading M, Wilburn FW. Chapter 5 – differential thermal analysis and differential scanning calorimetry. In: Brown ME, ed. *Handbook of Thermal Analysis and Calorimetry*. Elsevier Science B.V.; 1998:279-361.
22. Craver CD, Society C. *The Coblentz Society Desk Book of Infrared Spectra*. The Society; 1982.
23. Trautz M. Das Gesetz der Reaktionsgeschwindigkeit und der Gleichgewichte in Gasen. Bestätigung der Additivität von Cv-3/2R. Neue Bestimmung der Integrationskonstanten und der Moleküldurchmesser. *Z Anorg Allg Chem*. 1916;96(1):1-28.
24. Lewis WCM. XLI.—Studies in catalysis. Part IX. The calculation in absolute measure of velocity constants and equilibrium constants in gaseous systems. *J Chem Soc Trans*. 1918;113:471-492.

How to cite this article: Setter R, Schmölzer S, Rudolph N, Moukhina E, Wudy K. Thermal stability and curing behavior of acrylate photopolymers for additive manufacturing. *Polym Eng Sci*. 2023;63(7):2180-2192. doi:10.1002/pen.26355

APPENDIX A

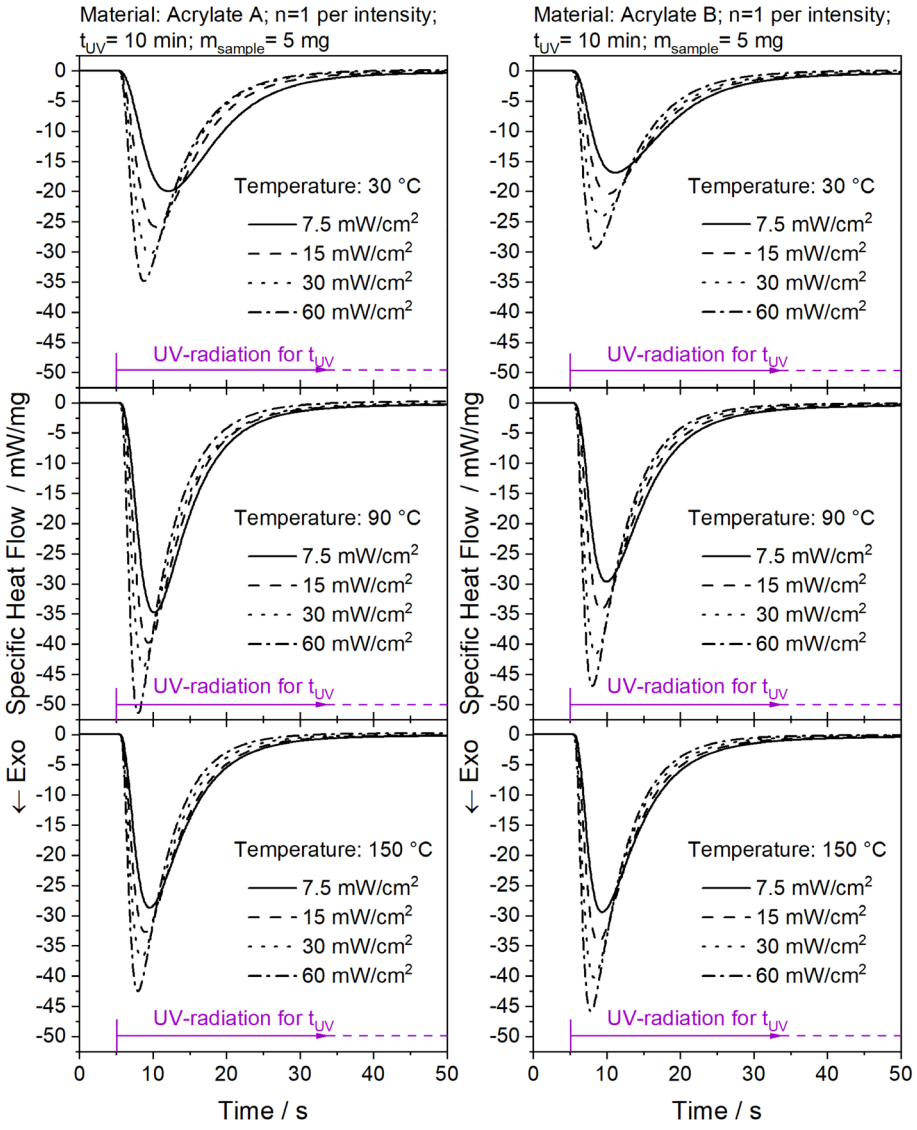

FIGURE A1 Comprehensive UV-DSC results for Acrylate A and B for different UV-intensities and temperatures.